



## Review paper

# Computer-aided diagnosis of congestive heart failure using ECG signals – A review



V. Jahmunah<sup>a,\*</sup>, Shu Lih Oh<sup>a</sup>, Joel Koh En Wei<sup>a</sup>, Edward J Ciaccio<sup>e</sup>, Kuang Chua<sup>a</sup>, Tan Ru San<sup>b</sup>, U. Rajendra Acharya<sup>a,c,d,1</sup>

<sup>a</sup> Department of Electronics and Computer Engineering, Ngee Ann Polytechnic, Singapore

<sup>b</sup> National Heart Centre, Singapore

<sup>c</sup> Department of Biomedical Engineering, School of Science and Technology, Singapore University of Social Sciences, Singapore

<sup>d</sup> School of Medicine, Faculty of Health and Medical Sciences, Taylor's University, 47500 Subang Jaya, Malaysia

<sup>e</sup> Department of Medicine – Cardiology, Columbia University, USA

## ARTICLE INFO

## Keywords:

Computer-aided detection system  
Congestive heart failure  
Deep learning  
Machine learning  
Statistical analysis

## ABSTRACT

The heart muscle pumps blood to vital organs, which is indispensable for human life. Congestive heart failure (CHF) is characterized by the inability of the heart to pump blood adequately throughout the body without an increase in intracardiac pressure. The symptoms include lung and peripheral congestion, leading to breathing difficulty and swollen limbs, dizziness from reduced delivery of blood to the brain, as well as arrhythmia. Coronary artery disease, myocardial infarction, and medical co-morbidities such as kidney disease, diabetes, and high blood pressure all take a toll on the heart and can impair myocardial function. CHF prevalence is growing worldwide. It afflicts millions of people globally, and is a leading cause of death. Hence, proper diagnosis, monitoring and management are imperative. The importance of an objective CHF diagnostic tool cannot be overemphasized. Standard diagnostic tests for CHF include chest X-ray, magnetic resonance imaging (MRI), nuclear imaging, echocardiography, and invasive angiography. However, these methods are costly, time-consuming, and they can be operator-dependent. Electrocardiography (ECG) is inexpensive and widely accessible, but ECG changes are typically not specific for CHF diagnosis. A properly designed computer-aided detection (CAD) system for CHF, based on the ECG, would potentially reduce subjectivity and provide quantitative assessment for informed decision-making. Herein, we review existing CAD for automatic CHF diagnosis, and highlight the development of an ECG-based CAD diagnostic system that employs deep learning algorithms to automatically detect CHF.

## 1. Introduction

Approximately 26 million adults worldwide suffer congestive heart failure (CHF) [1], which is a burgeoning healthcare problem [2]. Besides being a primary cause of death, CHF is also universally becoming a main cause of morbidity [3]. 70% of CHF cases are caused by cardiovascular ailments such as coronary artery disease [4]. Other causes of CHF include an elevated hemodynamic load, dysfunction related to ischemia, adverse ventricular remodeling, and genetic mutations [5]. Regardless of the etiology, early detection of CHF to avert further structural or functional impairment to the heart is imperative, and can save lives.

CHF is a chronic illness that affects the heart chambers. It occurs

when the heart is unable to pump blood adequately throughout the body without an increase in intracardiac pressure. The kidneys respond by retaining body fluid, which results in lung congestion and swelling in the arms and legs. CHF is caused by functional impairment of the left ventricle (LV), which is the dominant contractile chamber that pumps blood systemically. The systolic contractile function of the LV is conventionally quantitated using the LV ejection fraction (EF), defined as the ratio of LV stroke and end-diastolic volumes, with normal LVEF being 50% or more. CHF can be stratified into two main types: heart failure with reduced (HFrEF) and preserved EF (HFpEF) ejection fraction, characterized by predominance of either inadequate LV systolic contraction (EF less than 50% typically) or inability of the LV to expand or fill efficiently during diastole, respectively. While classification of

\* Corresponding author.

E-mail addresses: [e0145834@u.nus.edu](mailto:e0145834@u.nus.edu) (V. Jahmunah), [aru@np.edu.sg](mailto:aru@np.edu.sg) (U. R. Acharya).

<sup>1</sup> Postal address: Department of Electronics and Computer Engineering, Ngee Ann Polytechnic, Singapore 599489, Singapore.

HFrEF and HFpEF is arbitrarily based on the level of EF, elements of LV, both systolic contractile and diastolic filling pathophysiological changes, can co-exist in the same patient. Particularly in HFpEF, where LVEF is normal by definition, cardiac morphological and structural abnormalities offer important diagnostic clues. For instance, the presence of increased LV wall thickness or LV hypertrophy (LVH) and left atrial dilatation may signal increased LV wall stress and LV filling pressures, respectively. In both HFrEF and HFpEF, structural and/or functional perturbations cause raised intracardiac pressure with resultant lung and peripheral congestion, and/or diminished cardiac output, which compromises systemic perfusion to the organs [6]. In such a state, the LV needs to be steadily monitored for disease progression as well as response to therapy.

Accurate diagnosis and prognostication of CHF is obligatory. The functional severity of CHF can be qualitatively assessed using the New York Heart Association (NYHA) class [7]. In **Class 1**, physical activity is not hampered and normal physical activity does not cause symptoms. In **Class 2**, physical activity is noticeably limited, and less than ordinary activity causes heart failure symptoms. In **Classes 3 and 4**, patients experience heart failure symptoms with minimal physical activity or while resting, respectively. Analogous to cancer, CHF can also be staged [7]. In **Stage A and B**, patients are asymptomatic, but respectively have either risk factors (e.g. diabetes) or cardiac structural changes that predispose to developing heart failure. **Stages C and D** represent symptomatic and advanced refractory clinical heart failure, respectively. Both functional class and stage are helpful to clinically stratify patients for prognostication.

The importance of an objective CHF diagnostic tool cannot be overemphasized. Standard diagnostic tests for CHF include chest X-ray, magnetic resonance imaging (MRI), nuclear imaging, echocardiography, and invasive angiography, which can be time consuming and costly [8]. Of these, echocardiography is the one test most commonly utilized to assess heart structure and function in CHF, but the technique is especially operator-dependent. Computational methods using spatio-temporal statistical models may be employed to facilitate disease recognition [9], and potentially improve the interobserver reproducibility.

The electrocardiogram (ECG) is a crucial bio signal acquired via electrodes attached to the skin surface that represents the spatio-temporal electrical activity of the heart [10]. Electrocardiography (ECG) is inexpensive and widely accessible. The ECG may be subtly altered in CHF, but any alterations from normal are not specific for CHF diagnosis, typically due to subjectivity in the interpretation, and contamination by noise. The latter can be attributable to noise from poor electrode contact, interruption by power line frequency, and interference by electromyographic signals [11,12]. Additionally, it is challenging to decipher minute changes in the ECG signal, as its amplitude is measured in millivolts. All of these factors compromise the ability to detect slight changes in amplitude by visual inspection. Not surprisingly, manual examination of the ECG signal by clinicians is onerous and subject to intra- and interobserver variability. We believe that a well-designed computer-aided detection (CAD) system for CHF based on ECG, that considers and overcomes the problems stated herein, can potentially reduce subjectivity and provide accurate CHF diagnosis, as well as quantitative assessment for informed decision-making. A robust yet affordable diagnostic tool can be implemented in healthcare settings for assistance with CHF classification.

Herein, we review the existing CAD for automatic CHF diagnosis, and highlight the development of an ECG-based CAD diagnostic system that employs deep learning algorithms to automatically detect CHF. A typical CAD system comprises four key procedures: preprocessing of signals, extraction of unique features, selection of significant features, and classification. In this article, we emphasize the classification system that we have developed.

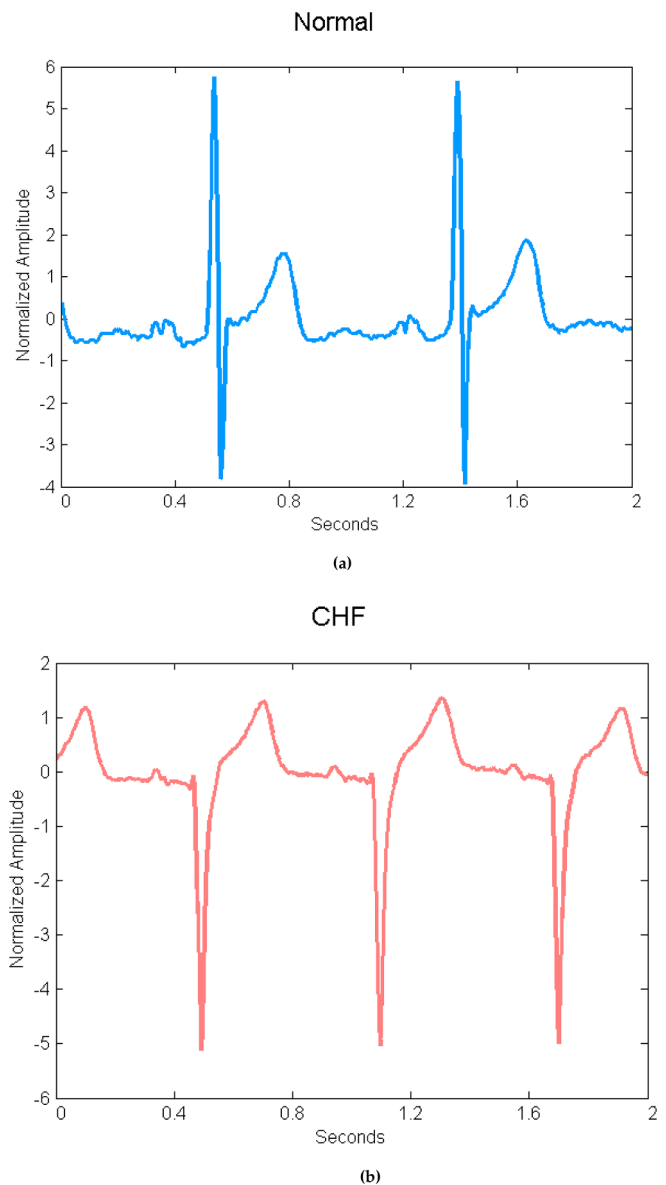


Fig. 1. Representation of normal ECG (a) and CHF ECG signal (b).

## 2. Data acquisition

The ECG signal is reflective of heart condition [13]. In some CHF patients, the ECG may demonstrate a high precordial QRS voltage or poor R wave progression, due to LV remodeling. A poor R wave progression occurs when there is a lack of the usual increase in the size of the R wave in the precordial leads from lead V1 to V6. Fig. 1 demonstrates a normal ECG signal and the ECG signal of a CHF patient. Fig. 2 represents the normal HRV signal and a heart rate variability (HRV) signal from a CHF patient.

### (i) ECG and HRV signals

The data used for analysis in this study included 803 HRV and 30,000 ECG signal segments obtained from 15 CHF patients with severe congestive failure (NYHA class 3–4) from the Beth Israel Deaconess Medical Center (BIDMC) Congestive Heart Failure database. Additionally, 855 HRV and 70,308 ECG signal segments were retrieved from 18 healthy subjects using the MIT-BIH Normal Sinus Rhythm (NSRDB) database [14].

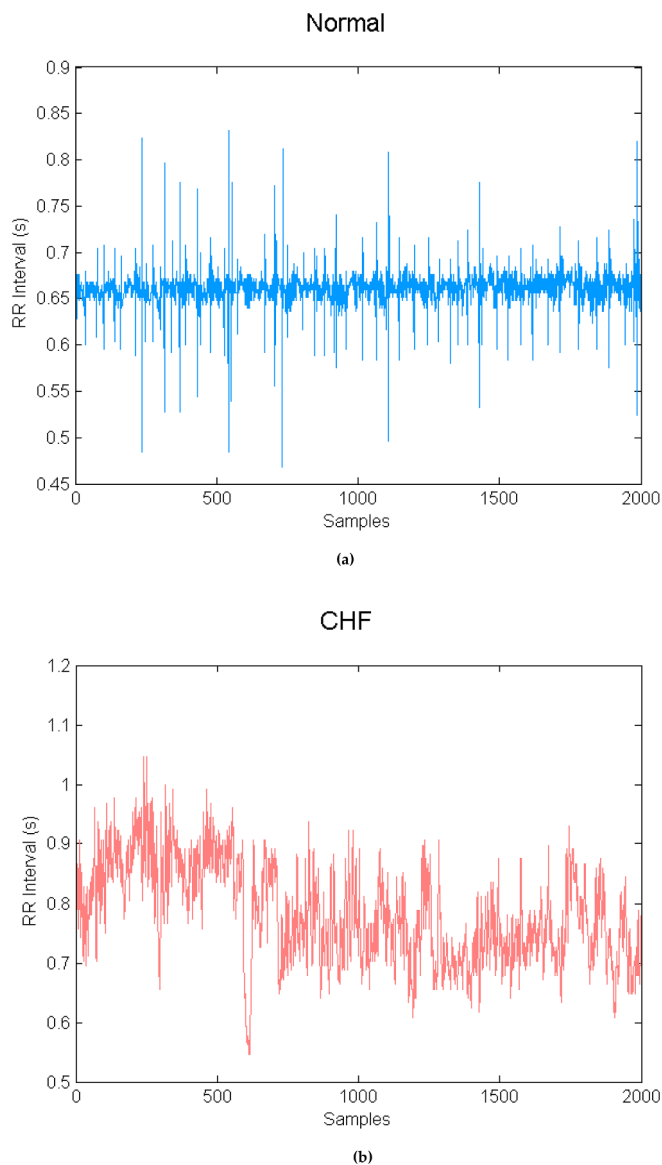


Fig. 2. Representation of normal HRV (a) and CHF HRV signal (b).

### (ii) Pre-processing

The ECG signals from the NSRDB and BIDMC databases were sampled at a frequency of 250 Hz, so that the frequency of the signals is consistent. The signals were then segmented into 2-second ECG segments without R peak detection. Z-score normalization was then applied to each segment [15,16]. Each HRV data was cut into a length of 2000 samples.

### (iii) Feature extraction

Highly distinct features were then extracted from the signals. Since HRV is represented by the R-R interval, the difference between heartbeats with respect to time and ECG signals will be time-varying and chaotic [17]. Hence, nonlinear features were studied.

## 3. Analysis

Nineteen nonlinear features were extracted from both signal types. These are the Approximate Entropy, Sample Entropy, Tsallis Entropy, Fuzzy Entropy, Kolmogorov Sinai Entropy, Modified Multi Scale

Entropy, Permutation Entropy, Rényi Entropy, Shannon Entropy, Wavelet Entropy, Kolmogorov Complexity, Lempel-Ziv Complexity, Signal Activity, Hjorth Complexity and mobility, Recurrence Qualitative Analysis, Largest Lyapunov Exponent, Correlation Dimension, Bispectrum and Cumulant features [17–39].

### (i) Approximate Entropy (ApEn)

ApEn is an algorithm proficient for computing uniformity and intricacy in time-series data that contain noise. Due to its capacity to differentiate interrelated stochastic processes and models, it is commonly used to study the ECG and electroencephalographic signals, as well as endocrine hormone secretion. It is useful to differentiate between noisy and chaotic time series within fairly short data intervals [18].

### (ii) Sample Entropy (SampEn)

SampEn is a statistical computation that is used to estimate the intricacy of biological time-series signals. It is an alternative to entropy estimation. Richman and Moorman mooted ‘SampEn’ as a means to measure the complexity of a system and to evaluate biomedical signals that identify noise easily [19]. The correlation integral  $C_m, i(> r)$ , represents the fraction of points within a distance  $r$ , from the  $i$ th point, when the signal is fixed in an  $m$ -dimensional space.

### (iii) Tsallis Entropy (Sq)

Sq is based upon Tsallis’ thermostatics, which is a standard used for statistical computation [20]. The Tsallis entropy is the foundation of statistical mechanics, which generalizes the Boltzmann-Gibbs theory. The Tsallis’ normalized probability distribution is obtained by following the MaxEnt route [21]. Sq, which has been used widely in diverse disciplines such as medicine and physics, is explored further in this paper, following.

### (iv) Fuzzy entropy

The measure of a quantity of fuzzy data gained from a fuzzy set or system is known as the Fuzzy entropy [22]. In Fuzzy entropy, the amount of uncertainty is assumed as a measure of information. Fuzzy entropy comprises vagueness and ambiguity uncertainties and is well-defined using the idea of a membership function [23].

### (v) Kolmogorov Sinai Entropy (KS entropy)

The KS entropy is a parameter used to enumerate chaos, for solving problems in complex systems. It is employed to measure the ambiguity of a system, linked to a series of outcomes or observations of chaotic trajectories after  $m$  units of time [24].

### (vi) Modified Multi Scale Entropy (MMSE)

The MMSE is an algorithm that is predominantly used to measure the intricacy of time series. This computation involves two processes; the derivation of a system is represented on different time scales by conducting a moving-averaging procedure and the consistencies of the moving-averages time series at a scale of  $\tau$  by applying SampEn with a time delay  $\tau$  [25].

### (vii) Permutation Entropy (PeEn)

Permutation entropy is a measure of the complexity of a system, derived from dynamical systems theory. PeEn has advantages including robustness and a nearly effortless calculation for chaotic and noisy time series. Permutation entropy is computed by selecting all possible data

sequences of length  $n$  and comparing them with all possible permutation patterns of  $n$  members that represent the rank orders of data values [26].

(viii) Rényi entropy

The Rényi entropy is considered to be a generalisation of Shannon's entropy for distinct variables. The  $p$ th Rényi entropy, which is defined as the entropy power, is the ordinary continuation of Shannon's entropy power. [27].

(ix) Shannon entropy

Shannon entropy is a shared information measure that is operated in the interdisciplinary registration of medical images. According to Shannon, the calculation of the amount of information  $H(p)$  contained in a sequence of events ( $p1...pN$ ) must fulfil three principles:  $H$  having to be continuous in the ( $p_i$ ), if ( $p_i$ ) =  $1/N$ , then  $H$  has to be a monotonic accumulative function of  $N$ , and  $H$  should be produced by addition [28].

(x) Wavelet Entropy (WE)

WE is a parameter with the ability to examine brief features of non-stationary signals. It combines wavelet decomposition and entropy to gauge the extent of disorder in a signal with high time–frequency resolution. Wavelet entropy has been extensively used to study physiological signals, such as the ECG and EEG, to obtain clinically valuable information [29].

(xi) Kolmogorov complexity

Andrey Kolmogorov developed the Kolmogorov complexity, an algorithmic approach to the quantitative interpretation of information. Kolmogorov complexity refers to the intricacy of a pattern that uses parameters to describe its occurrence, as the shortest algorithm required to produce it. It represents the compressibility of data, and is a feature that can be used to describe a system linearly or non-linearly [30].

(xii) Lempel-Ziv complexity (LZ complexity)

LZ complexity is a complexity measure which is the basis of the LZ77 compression algorithm. This measure considers the number of different patterns within a sequence, when examined from left to right, and is used to test the uncertainty of the sequence [31].

(xiii) Signal activity

Activity refers to the variance( $var$ ) of the time function. The computational value is small or large depending on the existence of few or large numbers of high frequency components, respectively. Activity is represented by the following equation,

$$Activity = var(y(t))$$

whereby  $y(t)$  represents the signal [32].

(xiv) Hjorth complexity and mobility

Mobility refers to the square root of the ratio of the variance of the signal and the variance of the first derivative of the signal [33].

Complexity characterizes the change in frequency of the signal. It shows how the shape of a signal is akin to that of a typical sine wave. The value of complexity approaches unity when the shape of the signal appears to be more like that of an actual sine wave [34].

(xv) Recurrence Qualitative Analysis(RQA)

RQA is an algorithm that emphasizes derived measures of the principle structural elements evident in recurrence plots. The diagonal lines are of paramount interest in distinguishing episodic components in time-series data, as their spreading and period are indicative of the copiousness and timing of periodic signal components [35].

(xvi) Largest Lyapunov Exponent (LLE)

LLE is a nonlinear parameter used to compute the sensitivity to initial conditions. It is the crucial invariant for identifying and characterizing chaos produced from a dynamical system. LLE is commonly used to study chaotic dynamics from time series [36].

(xvii) Correlation Dimension (CD)

The CD parameter stems from chaos theory and is a measure of the amount of multidimensional intricacy of an object. CD is a measure of the amount of space occupied by a set of random points [37].

(xviii) Bispectrum

The bispectrum is a Higher Order Spectra(HOS) feature that stems from the decomposition of the irregularity of a signal over frequency. The bispectrum only provides information in cases where the random process has a lopsided distribution, and has been shown to be potent in analyzing systems with uneven nonlinearities [38].

(xix) Cumulant

The cumulant is described as a moment, whereby the dependence on moments of lower order is eliminated. Cumulants are also known as the coefficients of the Taylor series expansion of the ordinary logarithm [39]. Cumulants are efficacious in analyzing imaginary signals [40].

#### 4. Results

The results of the above-mentioned features extracted from ECG signals and HRV signals are presented in Tables 1 and 2, respectively (refer to the Appendix). Fig. 3 represents the boxplot of the ten best features extracted from ECG signals, and Fig. 4 represents those extracted from HRV signals. Additionally, Figs. 5 and 6 signify the Cumulant plots for the ECG and HRV signals, respectively. From the results obtained, the mean of the entropy features extracted from ECG signals are lower in the CHF group as compared to that of the normal group. This could be attributed to a lower variability in the CHF group with respect to the healthy group. It is also evident that the t-values generated are higher in ECG signals as compared to HRV signals, due to the highly discriminatory nature of the features used. The boxplot in Fig. 3 highlighting the ECG, demonstrates that the values of some features such as the Kolmogorov complexity and entropy are higher for the normal class than that of CHF, owing to higher variability in the normal class. The same trend continues in Fig. 4, whereby features such as the Shannon and Rényi entropy portray to have higher values in the normal class as compared to CHF in the HRV signals. It is apparent that these plots are unique; hence it may be efficacious to use the features highlighted to differentiate the two classes.

#### 5. Discussion

Table 3 presents a summary of the studies of CAD systems using ECG for the classification of CHF. Table 4 highlights the summarized studies for CAD systems using HRV to classify CHF. It is notable that mainly transformational methods, coupled with entropy features, have been used by researchers in both studies to classify CHF. These methods

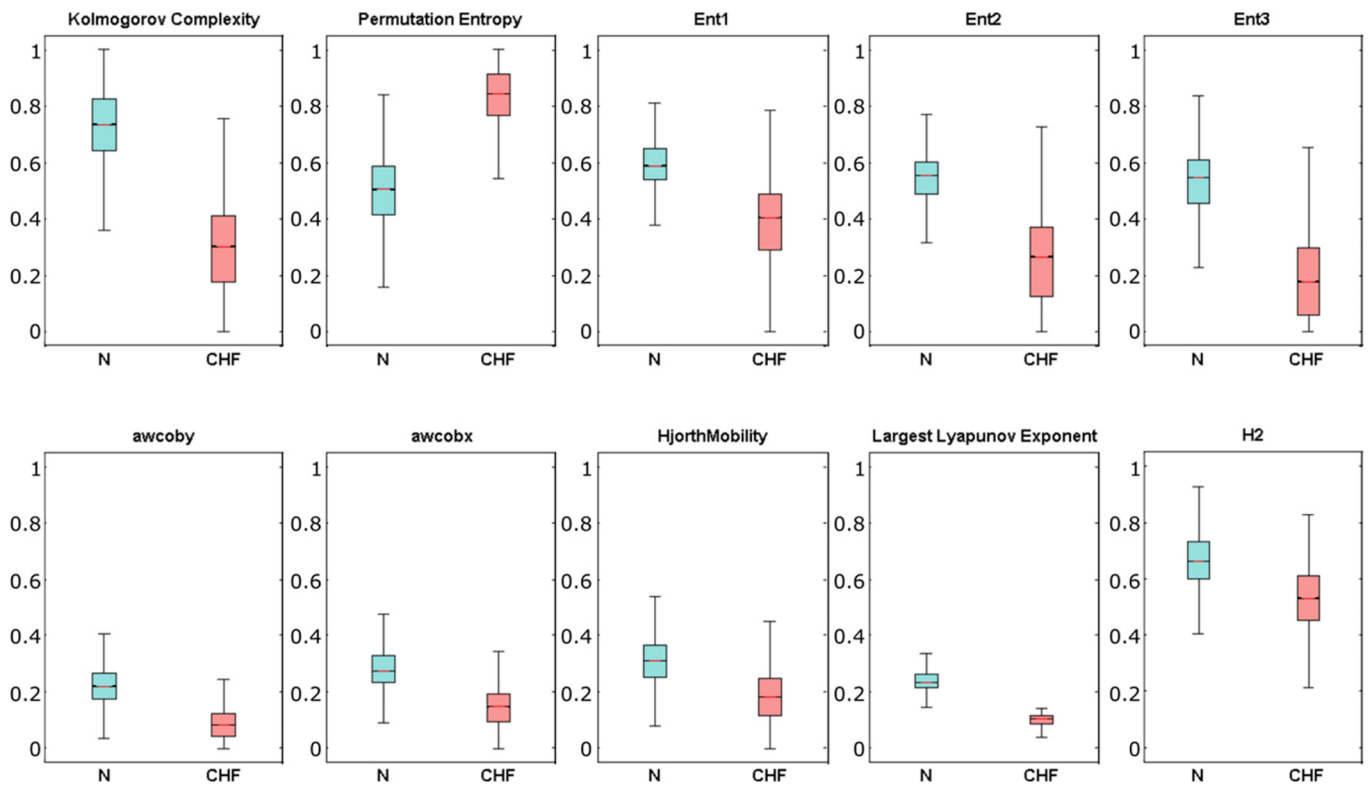


Fig. 3. Boxplot of features extracted from ECG signals.

enable the conversion of time to frequency domain signals. Additionally, SVM classifiers have been utilized extensively to aid in classification. The SVM is commonly used for classification due to its versatility in performing well with small data pools, where there is no overfitting, and in capturing non-linearity in features with its kernel

functions. Amongst other parameters, Acharya et al. [41] manipulated Shannon and Tsallis entropy features together with other parameters such as contourlet and shearlet coefficients, while Bhurane et al. [42] exploited Fuzzy, Rényi and Kraskov entropies coupled with the Quadratic Support Vector Machine. Both studies yielded high accuracies of

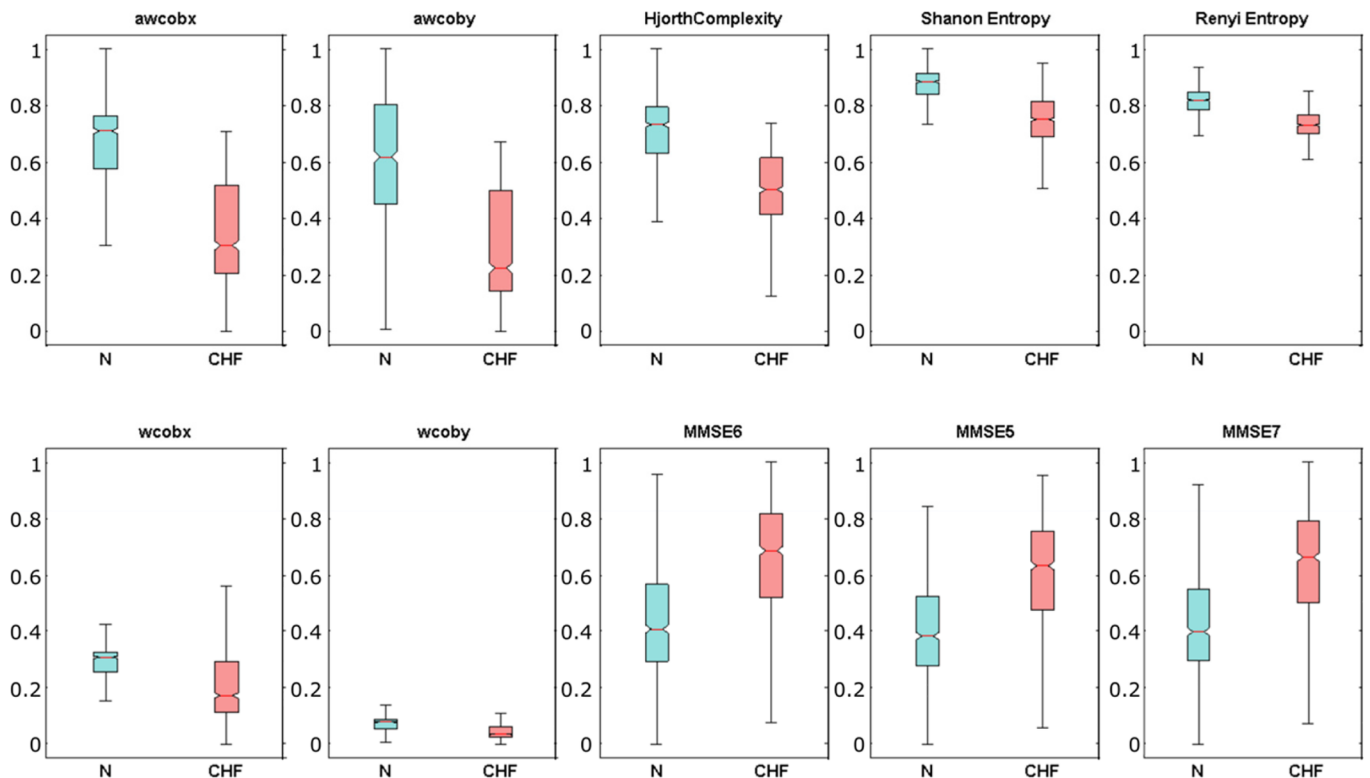


Fig. 4. Boxplot of features extracted from HRV signals.

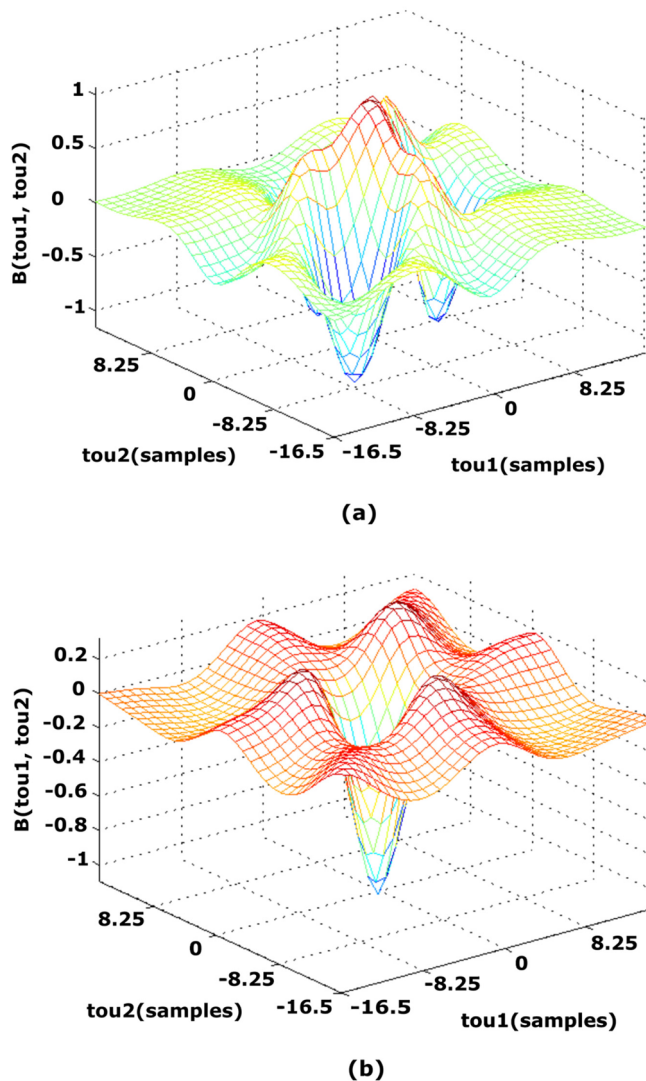


Fig. 5. A presentation of Cumulant plots for normal (a) and CHF (b) ECG signals, respectively.

99.01%, 99.95%, and > 99.66%, respectively. Furthermore, Liao et al. [43] and Bhurane et al. [42] operated with Support Vector Machines, generating accurate results. Pecchia et al. [44] employed time and frequency domain features and achieved an accuracy of 96.40%, while Yu et al. [45] used time, frequency domain and spectral features, coupled with SVM, and attained a classification accuracy of 98.79%. Liu et al. [46] and Shahbazi et al. [47] studied time and frequency domain features coupled with nonlinear features, and achieved classification accuracies of 100% each. These results are a testament to the transformational methods, yielding promising results when combined with nonlinear or entropy features.

However, machine learning techniques only perform well with small and balanced data. It should be noted that in reality, the existence of normal data is more, contributing to imbalanced data. With such skewed data, classification accuracy plummets. Additionally, features need to be extracted based on ‘trial and error’, until the optimal classification accuracy is achieved. To mitigate this problem, deep learning algorithms should be explored in future work.

## 6. Final remarks

Although clinical methods are becoming more accurate in the diagnosis of CHF, these methods still harbor some limitations.

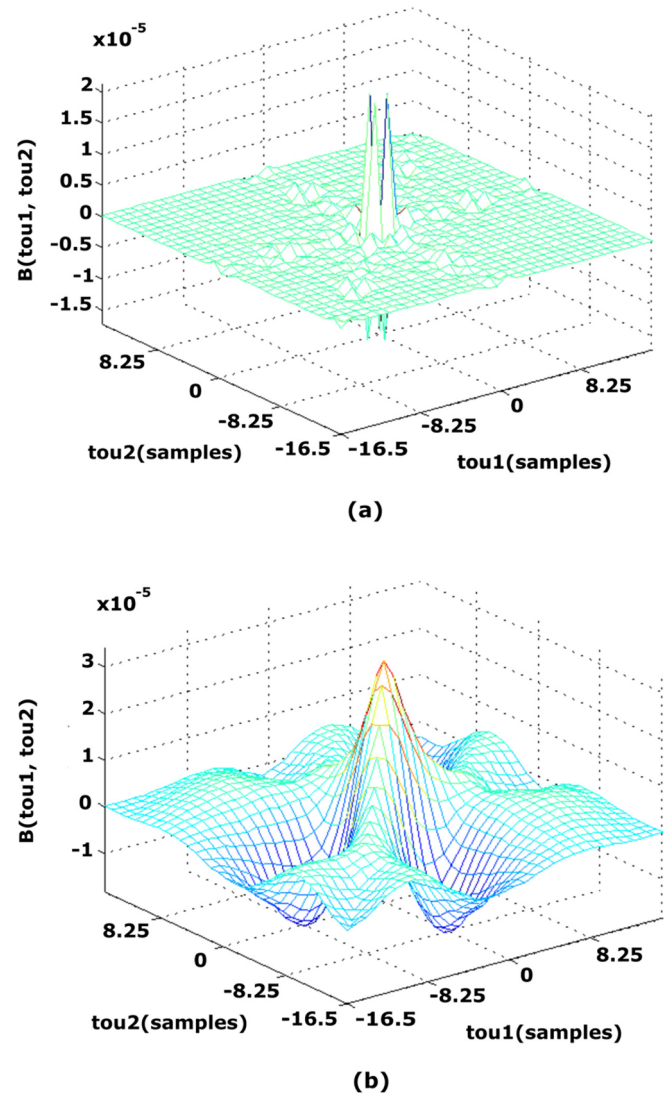


Fig. 6. A presentation of Cumulant plots for normal (a) and CHF (b) HRV signals, respectively.

Furthermore, these traditional methods are time-consuming, and the interpretation of ECG signals varies from one clinician to another. Hence, CAD systems that are noninvasive yet precise are currently of interest to diagnose the disease. This review paper provides evidence for increased benefit in using entropy and nonlinear features for the automated diagnosis of CHF with ECG signals. The performance of CAD systems may be improved by using cutting-edge deep learning paradigms[65].

Deep learning is a type of machine learning technique, which is more advanced as it learns large data, and selects distinct characteristics automatically based on the input ECG signals. The Artificial Neural Network (ANN) is a fundamental part of the deep learning model. ANN constitutes artificial neurons that imitate real neurons. The ANN structure contains a masked layer of hidden neurons between the input and output layers, which enables the extraction of higher-order statistics. The network learns from its environment as it undergoes the training process via the back-propagation algorithm[66]. The algorithm works by reducing error until the training data is considered learnt by the ANN [67].

The convolutional neural network (CNN) is an intricate structure which comprises many masked deep layers and parameters. It undergoes training, whereby kernels of various sizes are used to interpret the input data. CNN encompasses four main stages: the convolution stage

**Table 3**  
Summary of CAD systems using ECG for the classification of CHF.

Authors	Number of features	Techniques	Number of participants	Conclusion
Orhan et al. [48] 2013	–	<ul style="list-style-type: none"> <li>■ Equal frequency in amplitude and equal width in time discretization</li> </ul>	Normal: 18 subjects CHF: 15 patients	Sen: 99.36% Spe : 99.30%
Masetic et al. [49] 2013	–	<ul style="list-style-type: none"> <li>■ The Burg method for autoregressive (AR) parameter estimation</li> <li>■ Random Forest Classifier</li> </ul>	Normal: 13 subjects CHF1st dataset: 15 patients, 2nd dataset: 3 patients	Acc: 100% Sen: 100% Spe : 100%
Kamath et al. [50] 2015	45	<ul style="list-style-type: none"> <li>■ Detrended Fluctuation Analysis(DFA)</li> </ul>	Normal: 58 subjects CHF: 15 patients	Acc: 99.20% Sen: 98.40% Spe : 98.00%
Liao et al. [43] 2015	Input features in multiples of 64	<ul style="list-style-type: none"> <li>■ ECG unit patterns(64 samples each)</li> <li>■ C and Gamma parameters</li> <li>■ SVM classifier</li> </ul>	Normal: 18 subjects CHF: 15 patients	Acc: 97.27%
Vidya et al. [51] 2017	24	<ul style="list-style-type: none"> <li>■ Dual tree complex wavelet transform(DTCWT)</li> <li>■ Statistical features               <ul style="list-style-type: none"> <li>o Maximum</li> <li>o Minimum</li> <li>o Mean</li> <li>o Standard deviation</li> </ul> </li> <li>■ Median</li> </ul>		Acc: 99.86% Sen: 99.78% Spe : 99.94%
Acharya et al. [41] 2017	20 (ANOVA), 20 (Relieff)	<ul style="list-style-type: none"> <li>■ Contourlet and shearlet coefficients</li> <li>■ Mean, min, max, standard deviation, average power, inter-quartile range, Shannon entropy, mean Tsallis entropy kurtosis, mean absolute deviation, mean energy</li> <li>■ IBPSO</li> <li>■ ANOVA, Relieff</li> <li>■ DT, kNN</li> </ul>	Normal: 52 subjects CAD: 7 patients, MI: 148 patients, CHF: 15 patients	Contourlet transform Acc: 99.95% Sen: 99.93% Spe : 99.24% Shearlet transform Acc: 99.01% Sen: 99.82% Spe: 98.75%
Acharya et al. [52] 2018	–	<ul style="list-style-type: none"> <li>■ kNN classifier</li> <li>■ 11-layered deep learning model(CNN)</li> </ul>	Normal: 58 subjects CHF: 15 patients	Dataset B: Sen: 98.87% Spe: 99.01% Acc: 98.97%
Faust et al. [53] 2018	–	<ul style="list-style-type: none"> <li>■ RNN with LSTM</li> <li>■ 10-fold cross validation</li> <li>■ Blindfold validation</li> <li>■ LSTM classifier</li> </ul>	AF: 20 patients(10-fold), 3 patients(blindfold)	10-fold validation Acc: 98.51% Sen: 98.32% Spe: 98.67% Positive predictive accuracy: 98.39% Blindfold validation Acc: 99.77% Sen: 99.87% Spe: 99.61% Positive predictive accuracy: 99.72%
Kumar et al. [54] 2018	3	<ul style="list-style-type: none"> <li>■ Decomposition of ECG signals using scaling and wavelet coefficients.</li> <li>■ Down-sampling by scaling and wavelet filter banks</li> <li>■ Biorthogonal wavelet transform</li> <li>■ MATLAB R2017a</li> </ul>	Normal: 68 subjects CHF: 15 patients Myocardial infarction: 148 Coronary artery disease:7	Classification of healthy, CHF, myocardial infarction and coronary artery disease: Acc: 99.92% Sen: 99.94% Spe: 99.92% Error: 0.0013
Sharma et al. [55] 2018	–	<ul style="list-style-type: none"> <li>■ Eigenvalue decomposition of Hankel matrix for removal of baseline wander and power line interference</li> <li>■ K-mean clustering</li> </ul>	Normal:2 Premature ventricular contraction: 1	Proposed method performs better compared to existing methods that use performance indicators such as output signal to noise ratio percent root mean square difference, for pre-processing ECG signals.
Bhurane et al. [42] 2019	5	<ul style="list-style-type: none"> <li>■ Fuzzy entropy</li> <li>■ Rényi entropy</li> <li>■ Higuchi Fractal Dimension</li> <li>■ Kraskov entropy, energy</li> <li>■ Frequency localised filter banks</li> <li>■ Quadratic support vector machine(QSVM)</li> <li>■ 10-fold cross validation</li> </ul>	Fantasia: 40 healthy subjects, NSRDB: 18 healthy subjects, BIDMC: 18 CHF patients.	Acc: > 99.66% Sen: > 99.82% Spe: > 99.28%

where features are extracted from the input signals, the rectified linear activation stage where non-linearity in the data is charted, the pooling stage where features and computational complexities are reduced, and the fully-connected layer that sorts the input data into various classes according to the data used for training [68]. In recent times, CNN has been used successfully to detect heart diseases [69], and it is employed for such purposes as diagnosing arrhythmias [70–72] myocardial infarction [73,74] and atrial fibrillation [75,53]. It has also been explored in differentiating the ECG signals observed in coronary artery disease from normal signals [4], and in detecting shockable versus non-shockable ventricular arrhythmias[76]. A long short-term memory

(LSTM) coupled with CNN has also been employed to effectively diagnose coronary artery disease with an accuracy of 99.85%[77]. Hence, in future manifestations of the system, we believe that a deep learning system could be implemented in CAD to study ECG signals, for the successful detection of CHF. Furthermore, this system could be used as a supplementary tool to aid clinicians in delivering better and more accurate diagnostic information to patients[78].

## 7. Conclusion

CHF is a complex clinical condition in which the capacity of the

**Table 4**  
Summary of CAD systems using HRV for the classification of CHF.

Authors	Number of features	Techniques	Number of participants	Conclusion
Thuraisingham et al. [56] 2009	6	<ul style="list-style-type: none"> <li>■ Second order difference plot (SODP) features</li> </ul>	Normal: 36 subjects CHF: 36 patients	Acc: 100%
Pecchia et al. [44] 2011	9	<ul style="list-style-type: none"> <li>■ Time domain measure</li> <li>■ Frequency domain measure</li> </ul>	Normal: 54 subjects CHF: 29 patients	Acc: 96.40% Sen: 89.70% Spe: 100%
Jong et al. [57] 2011	–	<ul style="list-style-type: none"> <li>■ Detrended fluctuation analysis (DFA)</li> <li>■ Kruskal-Wallis test</li> </ul>	Normal: 54 subjects CHF: 29 patients	Acc: 96%
Yu et al. [45] 2012	42	<ul style="list-style-type: none"> <li>■ Time domain measures</li> <li>■ Frequency domain measures</li> <li>■ Bispectrum measures</li> <li>■ SVM classifier</li> </ul>	Normal: 54 subjects CHF: 29 patients	Acc: 98.79%
Melillo et al. [58], 2013	13	<ul style="list-style-type: none"> <li>● Time domain measures</li> <li>● Frequency domain measures</li> </ul>	CHF: 12 mild CHF, 32 severe CHF patients	Spe: 63.60% Sen: 93.30%
Liu et al. [46], 2014	12	<ul style="list-style-type: none"> <li>● Time domain measures</li> <li>● Frequency domain measures</li> <li>● Nonlinear measures</li> </ul>	Normal: 30 subjects CHF: 17 patients	Acc: 100% Sen: 100% Spe: 100%
Narin et al. [59], 2014	27	<ul style="list-style-type: none"> <li>● Time domain measures</li> <li>● Lomb- and fast Fourier transform (FFT)-based frequency domain measures</li> <li>● Wavelet-based measures</li> <li>● Nonlinear measures</li> <li>● SVM classifier</li> </ul>	Normal: 54 subjects CHF: 29 patients	Acc: 91.56% Sen: 82.75% Spe: 96.29%
Shahbazi et al. [47], 2015	–	<ul style="list-style-type: none"> <li>■ Time domain measures</li> <li>■ Frequency domain measures</li> <li>■ Nonlinear measures</li> </ul>	CHF: 12 mild CHF, 32 severe CHF patients	Sen: 100.00% Spe: 100.00%
Acharya et al. [60], 2016	5	<ul style="list-style-type: none"> <li>● Empirical mode decomposition (EMD)</li> <li>● Nonlinear measures</li> <li>● Kruskal-Wallis test</li> </ul>	Normal: 10 subjects CHF: 10 patients	Acc: 97.64% Sen: 80.00% Spe: 94.40%
Kumar et al. [61], 2017	2	<ul style="list-style-type: none"> <li>● Flexible analytic wavelet transform (FAWT)</li> <li>● Fuzzy entropy</li> <li>● Accumulated permutation entropy</li> </ul>	Normal: 58 subjects CHF: 15	500 sample length Acc: 98.21% Sen: 98.07% Spe: 98.33%
				1000 sample length Acc: 98.01% Sen: 97.95% Spe: 98.07%
				2000 sample length Acc: 97.71% Sen: 97.76% Spe: 97.67%
Feng et al. [62], 2019	–	<ul style="list-style-type: none"> <li>● Time domain indicators; standard deviation of the normal-to-normal (NN) intervals, root mean square of successive differences between adjacent NN intervals, percentage of NN intervals &gt; 50 ms, ratio of low frequency and low frequency.</li> <li>● Frequency domain indicators from very-high frequency, high frequency, low frequency and very-low frequency obtained.</li> <li>● Multi-frequency component analysis</li> <li>● T-test, Fisher discriminant, ANOVA test.</li> <li>● Eigenvalue decomposition of Hankel Matrix</li> <li>● Mean and standard deviation in time domain, mean frequency from Fourier-Bessel series expansion, k-nearest neighbour entropy, correntropy parameters.</li> <li>● Least-squares support vector machine classifier coupled with radial-basis function.</li> </ul>	Normal: 54 subjects Low-risk CHF: 12 High-risk CHF: 32	Acc (using MFC-En): 86.7% LF/HF ratio is 79.6%.
Sharma et al. [63], 2019	5	<ul style="list-style-type: none"> <li>● Long short-term memory coupled with convolution net deep network</li> <li>● Blindfold validation</li> <li>● 5 databases</li> </ul>	Normal: 112 subjects CHF: 44	Acc: 93.33% Sen: 91.41% Spe: 94.90%
Wang et al. [64], 2019	–	<ul style="list-style-type: none"> <li>● Long short-term memory coupled with convolution net deep network</li> <li>● Blindfold validation</li> <li>● 5 databases</li> </ul>	Beth Israel Deaconess Medical Center database: Severe CHF: 15 Congestive heart failure RR interval database: CHF: 29 Massachusetts Institute of Technology-Beth Israel Hospital normal sinus rhythm database: Normal: 18 subjects Normal sinus rhythm RR interval database: Normal: 54 subjects Fantasia database: Normal: 40 subjects	Beth Israel Deaconess Medical Center(CHF): Acc: 99.22% Normal sinus rhythm: Acc: 99.22% Fantasia: Acc: 98.92% NSR-RR & CHF-RR: Acc for RR segment(N = 500) : 82.52% Acc for RR segment(N = 1000) : 86.68% Acc for RR segment(N = 2000) : 87.55%

heart to fill and to pump blood is impaired due to functional or structural disease. Early detection of CHF is of high importance to avert death. This paper provides an overview of the existing CAD systems that have been developed to aid cardiologists in the diagnosis of CHF based on the widely available and inexpensive ECG signal. Detecting CHF using ECG-based CAD systems coupled with deep learning methods may be beneficial as compared to doing so via manual inspection of signals. The profound competency of deep learning is likely to boost classification performance when it is integrated into a CAD system. Thus, with the availability of larger datasets to train the model, these robust CAD systems have the potential to produce highly accurate and reliable diagnostic results.

## Appendix A. Supplementary data

Supplementary data to this article can be found online at <https://doi.org/10.1016/j.ejmp.2019.05.004>.

## References

- [1] Bui AL, Horwich TB, Fonarow GC. Epidemiology and risk profile of heart failure. *Nat Rev Cardiol* 2011;8:30–41. <https://doi.org/10.1038/nrcardio.2010.165>.
- [2] Ambrosy AP, Fonarow GC, Butler J, Chioncel O, Greene SJ, Vaduganathan M, et al. The global health and economic burden of hospitalizations for heart failure: lessons learned from hospitalized heart failure registries. *J Am Coll Cardiol* 2014;63:1123–33. <https://doi.org/10.1016/j.jacc.2013.11.053>.
- [3] Sakata Y, Shimokawa H. Epidemiology of heart failure in Asia. *Circ J* 2013;77:2209–17. <https://doi.org/10.1016/j.jhc.2015.07.009>.
- [4] Acharya UR, Fujita H, Lih OS, Adam M, Tan JH, Chua CK. Automated detection of coronary artery disease using different durations of ECG segments with convolutional neural network. *Knowledge-Based Syst* 2017;132:62–71. <https://doi.org/10.1016/j.knsys.2017.06.003>.
- [5] Burgess A, Shah K, Hough O, Hynynen K. *HHS Public Access* 2016;15:477–91. <https://doi.org/10.1586/14737175.2015.1028369.Focused>.
- [6] Hunt SA, Abraham WT, Chin MH, Feldman AM, Francis GS, Ganiats TG, et al. 2009 focused update incorporated into the ACC/AHA 2005 guidelines for the diagnosis and management of heart failure in adults. *J Am Coll Cardiol* 2009;53:e1–90. <https://doi.org/10.1016/j.jacc.2008.11.013>.
- [7] Inamdar AA, Inamdar AC. Heart failure : diagnosis, management and utilization. *J Clin Med* 2016. <https://doi.org/10.3390/jcm5070062>.
- [8] Gladding PA, Cave A, Zareian M, Smith K, Hussain J, Homer ML, et al. Personalized medicine open access integrated therapeutic and diagnostic platforms for personalized cardiovascular medicine. *J Pers Med* 2013;2:303–37. <https://doi.org/10.3390/jpm3030203>.
- [9] Beymer D, Syeda-Mahmood T. Cardiac disease recognition in echocardiograms using spatio-temporal statistical models. *Conf Proc Annu Int Conf IEEE Eng Med Biol Soc IEEE Eng Med Biol Soc Annu Conf* 2008;2008:4784–8. <https://doi.org/10.1109/IEMBS.2008.4650283>.
- [10] Baumert M, Porta A, Cichocki A. Biomedical signal processing: from a conceptual framework to clinical applications [Scanning the Issue]. *Proc IEEE* 2016;104:220–2. <https://doi.org/10.1109/JPROC.2015.2511359>.
- [11] Chang CH, Ko HJ, Chang KM. Cancellation of high-frequency noise in ECG signals using adaptive filter without external reference. *Proc - 2010 3rd Int Conf Biomed Eng Informatics BMEI*; 2010. p. 787–90. <https://doi.org/10.1109/BMEI.2010.5639953>.
- [12] Martis RJ, Acharya UR, Adeli H. Current methods in electrocardiogram characterization. *Comput Biol Med* 2014;48:133–49. <https://doi.org/10.1016/j.combiomed.2014.02.012>.
- [13] Rajendra Acharya U, Faust O, Adib Kadri N, Suri JS, Yu W. Automated identification of normal and diabetes heart rate signals using nonlinear measures. *Comput Biol Med* 2013;43:1523–9. <https://doi.org/10.1016/j.combiomed.2013.05.024>.
- [14] Goldberger AL, Amaral LAN, Glass L, Hausdorff JM, Ivanov PCh, Mark RG, et al. Current Perspective. *Circulation* 2000;101:215–20. <https://doi.org/10.1161/01.CIR.101.23.e215>.
- [15] Panda SK, Jana PK. SLA-based task scheduling algorithms for heterogeneous multi-cloud environment. *J Supercomput* 2017;73:2730–62. <https://doi.org/10.1007/s11227-016-1952-z>.
- [16] Panda SK, Jana PK. A multi-objective task scheduling algorithm for heterogeneous multi-cloud environment. *2015 Int Conf Electron Des Comput Networks Autom Verif EDCAV* 2015. p. 82–7. <https://doi.org/10.1109/EDCAV.2015.7060544>.
- [17] Faust O, Acharya UR, Krishnan SM, Min LC. Analysis of cardiac signals using spatial filling index and time-frequency domain. *Biomed Eng Online* 2004;3:1–11. <https://doi.org/10.1186/1475-925X-3-30>.
- [18] Pincus S. Approximate entropy (ApEn) as a complexity measure. *Chaos* 1995;5:110–7. <https://doi.org/10.1063/1.166092>.
- [19] Richman JS, Moorman JR. Physiological time-series analysis using approximate entropy and sample entropy. *Am J Physiol Circ Physiol* 2017;278:H2039–49. <https://doi.org/10.1152/ajpheart.2000.278.6.h2039>.
- [20] Anastasiadis A. Special issue: Tsallis entropy. *Entropy* 2012;14:174–6. <https://doi.org/10.3390/e14020174>.
- [21] Jaynes ET. *Principles of Statistical Mechanics-The Information Theory Approach*. 1968.
- [22] Ramer A. Concepts of fuzzy information measures on continuous domains. *Int J Gen Syst* 1990;17:241–8. <https://doi.org/10.1080/03081079008935109>.
- [23] Al-sharhan S, Karray F, Gueaieb W, Basir O. Fuzzy entropy: a brief survey. *10th. IEEE Int Conf Fuzzy Syst (Cat No01CH37297)* 2001;2:1135–9. <https://doi.org/10.1109/FUZZ.2001.1008855>.
- [24] Pham TD. The Kolmogorov-Sinai entropy in the setting of fuzzy sets for image texture analysis and classification. *Pattern Recogn* 2016;53:229–37. <https://doi.org/10.1016/j.patcog.2015.12.012>.
- [25] De WuS, Wu CW, Lee KY, Lin SG. Modified multiscale entropy for short-term time series analysis. *Phys A Stat Mech Its Appl* 2013;392:5865–73. <https://doi.org/10.1016/j.physa.2013.07.075>.
- [26] Dostál O, Vysata O, Pazdera L, Procházka A, Kopal J, Kuchyňka J, et al. Permutation entropy and signal energy increase the accuracy of neuropathic change detection in needle EMG. *Comput Intell Neurosci* 2018;2018. <https://doi.org/10.1155/2018/5276161>.
- [27] Savare G, Toscani G. The concavity of rényi entropy power. *IEEE Trans Inf Theory* 2014;60:2687–93. <https://doi.org/10.1109/TIT.2014.2309341>.
- [28] Shannon Claude E. A mathematical theory of communication. *Bell Syst Tech J* 1948;27:623–56. <https://doi.org/10.2307/3611062>.
- [29] Rosso OA, Blanco S, Yordanova J, Kolev V, Figliola A, Schürmann M, Başar E. Wavelet entropy: a new tool for analysis of short duration brain electrical signals. *J Neurosci Method* 2001;105:65–75. [https://doi.org/10.1016/S0165-0270\(00\)00356-3](https://doi.org/10.1016/S0165-0270(00)00356-3).
- [30] Kolmogorov AN. Three approaches to the quantitative definition of information. *Int J Comput Math* 1968;2:157–68. <https://doi.org/10.1080/00207166808803030>.
- [31] Ziv J, Lempel A. A universal algorithm for sequential data compression. *IEEE Trans Inf Theory* 1977;23:337–43. <https://doi.org/10.1109/TIT.1977.1055714>.
- [32] Sweller J. Introduction. *Educ Psychol Rev* 1988;12:257–85. [https://doi.org/10.1207/s15516709cog1202\\_4](https://doi.org/10.1207/s15516709cog1202_4).
- [33] Sweller J, Van Merriënboer JGG, Paas FGWC. Cognitive architecture and instructional design. *Educ Psychol Rev* 1998;10:251–96. <https://doi.org/10.1023/A:1022193728205>.
- [34] Brünken R, Plass JL. *Bruenken\_Plass\_Leutner\_EP* 2003. p. 1–9. [https://doi.org/10.1207/S15326985EP3801\\_7](https://doi.org/10.1207/S15326985EP3801_7).
- [35] Curtin P, Curtin A, Austin C, Gennings C, Tammimies K, Bölte S, et al. Recurrence quantification analysis to characterize cyclical components of environmental elemental exposures during fetal and postnatal development. *PLoS ONE* 2017;12:e0187049.
- [36] Pavlov AN, Pavlova ON, Kurths J. Determining the largest Lyapunov exponent of chaotic dynamics from sequences of interspike intervals contaminated by noise. *Eur Phys J B* 2017;90. <https://doi.org/10.1140/epjb/e2017-70439-7>.
- [37] Budescu B, Cälîman A, Ivanovici M. The correlation dimension: a video quality measure. *Lect Notes Inst Comput Sci Soc Telecommun Eng* 2012;79:55–64. [https://doi.org/10.1007/978-3-642-30419-4\\_5](https://doi.org/10.1007/978-3-642-30419-4_5).
- [38] Collis WB, White PR, Hammond JK. Higher-order spectra: the bispectrum and trispectrum. *Mech Syst Signal Process* 1998;12:375–94. <https://doi.org/10.1006/mssp.1997.0145>.
- [39] Brillinger DR. An introduction to polyspectra. *Ann Math Stat* 1965;36:1351–74. <https://doi.org/10.1214/aoms/1177699896>.
- [40] Brillinger DR. *Time Series: Data Analysis and Theory*. New York: McGraw-Hill; 1981.
- [41] Acharya UR, Fujita H, Sudarshan VK, Oh SL, Adam M, Tan JH, et al. Automated characterization of coronary artery disease, myocardial infarction, and congestive heart failure using contourlet and shearlet transforms of electrocardiogram signal. *Knowledge-Based Syst* 2017;132:156–66. <https://doi.org/10.1016/j.knsys.2017.06.026>.
- [42] Bhurane AA, Sharma M, San-Tan R, Rajendra Acharya U. An efficient detection of congestive heart failure using frequency localized filter banks for the diagnosis with ECG signals. *Cogn Syst Res* 2019;55:82–94. <https://doi.org/10.1016/j.cogsys.2018.12.017>.
- [43] Liao Ken Ying-Kai, Chiu Chuang-Chien, Yeh Shouu-Jeng. A novel approach for classification of congestive heart failure using relatively short-term ECG waveforms and SVM CLASSIFIER. *Proc Int MultiConference Eng Comput Sci* 2015, IMECS 2015, March 18–20, 2015, Hong Kong. 2015. p. 18–21.
- [44] Melillo P, Fusco R, Sansone M, Bracale M, Pecchia L. Discrimination power of long-term heart rate variability measures for chronic heart failure detection. *Med Biol Eng Comput* 2011;49:67–74. <https://doi.org/10.1007/s11517-010-0728-5>.
- [45] Yu SN, Lee MY. Bispectral analysis and genetic algorithm for congestive heart failure recognition based on heart rate variability. *Comput Biol Med* 2012;42:816–25. <https://doi.org/10.1016/j.combiomed.2012.06.005>.
- [46] Liu G, Wang L, Wang Q, Zhou GM, Wang Y, Jiang Q. A new approach to detect congestive heart failure using short-term heart rate variability measures. *PLoS ONE* 2014;9. <https://doi.org/10.1371/journal.pone.0093399>.
- [47] Shahbazi F, Asl BM. Generalized discriminant analysis for congestive heart failure risk assessment based on long-term heart rate variability. *Comput Methods Programs Biomed* 2015;122:191–8. <https://doi.org/10.1016/j.cmpb.2015.08.007>.
- [48] Orhan U. Real-time CHF detection from ECG signals using a novel discretization method. *Comput Biol Med* 2013;43:1556–62. <https://doi.org/10.1016/j.combiomed.2013.07.015>.
- [49] Mašetić Z, Subasi Abdulhamit. Detection of congestive heart failures using c4. 5 decision tree. *Southeast Eur J Soft Comput* 2013;2. <https://doi.org/10.21533/scjournal.v2i2.32>.
- [50] Kamath C. A new approach to detect congestive heart failure using detrended fluctuation analysis of electrocardiogram signals. *J Eng Sci Technol*

- 2015;10:145–59.
- [51] Sudarshan VK, Acharya UR, Lih S, Adam M, Hong J, Kuang C, et al. Automated diagnosis of congestive heart failure using dual tree complex wavelet transform and statistical features extracted from 2 s of ECG signals. *Comput Biol Med* 2017;83:48–58. <https://doi.org/10.1016/j.compbmed.2017.01.019>.
- [52] Acharya UR, Fujita H, Oh SL, Hagiwara Y, Tan JH, Adam M, et al. Deep convolutional neural network for the automated diagnosis of congestive heart failure using ECG signals. *Appl Intell* 2018. <https://doi.org/10.1007/s10489-018-1179-1>.
- [53] Faust O, Shenfield A, Kareem M, San TR, Fujita H, Acharya UR. Automated detection of atrial fibrillation using long short-term memory network with RR interval signals. *Comput Biol Med* 2018;102:327–35. <https://doi.org/10.1016/j.compbmed.2018.07.001>.
- [54] Kumar A, Komaragiri R, Kumar M. Heart rate monitoring and therapeutic devices: a wavelet transform based approach for the modeling and classification of congestive heart failure. *ISA Trans* 2018;79:239–50. <https://doi.org/10.1016/j.isatra.2018.05.003>.
- [55] Sharma RR, Pachori RB. Baseline wander and power line interference removal from ECG signals using eigenvalue decomposition. *Biomed Signal Process Control* 2018;45:33–49. <https://doi.org/10.1016/j.bspc.2018.05.002>.
- [56] Thuraisingham RA. A classification system to detect congestive heart failure using second-order difference plot of RR intervals. *Cardiol Res Pract* 2009;2009:1–7. <https://doi.org/10.4061/2009/807379>.
- [57] Jong TL, Chang B, Kuo CD. Optimal timing in screening patients with congestive heart failure and healthy subjects during circadian observation. *Ann Biomed Eng* 2011;39:835–49. <https://doi.org/10.1007/s10439-010-0180-6>.
- [58] Melillo P, De Luca N, Bracale M, Pecchia L. Classification tree for risk assessment in patients suffering from congestive heart failure via long-term heart rate variability. *IEEE J Biomed Heal Informatics* 2013;17:727–33. <https://doi.org/10.1109/JBHI.2013.2244902>.
- [59] Narin A, Isler Y, Ozer M. Investigating the performance improvement of HRV Indices in CHF using feature selection methods based on backward elimination and statistical significance. *Comput Biol Med* 2014;45:72–9. <https://doi.org/10.1016/j.compbmed.2013.11.016>.
- [60] Sood S, Kumar M, Pachori RB, Acharya UR. Application of empirical mode decomposition-based features for analysis of normal and Cad heart rate signals. *J Mech Med Biol* 2016;16:1640002. <https://doi.org/10.1142/S0219519416400029>.
- [61] Kumar M, Pachori RB, Acharya UR. Use of accumulated entropies for automated detection of congestive heart failure in flexible analytic wavelet transform framework based on short-term HRV signals. *Entropy* 2017;19. <https://doi.org/10.3390/e19030092>.
- [62] Pan W, He A, Feng K, Li Y, Wu D, Liu G. Multi-frequency components entropy as novel heart rate variability indices in congestive heart failure assessment. *IEEE Access* 2019. <https://doi.org/10.1109/access.2019.2896342>.
- [63] Sharma RR, Kumar A, Pachori RB, Acharya UR. Accurate automated detection of congestive heart failure using eigenvalue decomposition based features extracted from HRV signals. *Biocybern Biomed Eng* 2018. <https://doi.org/10.1016/j.bbe.2018.10.001>.
- [64] Wang L, Zhou X. Detection of congestive heart failure based on LSTM-based deep network via short-term RR intervals. *Sensors* 2019;19:1502. <https://doi.org/10.3390/s19071502>.
- [65] Faust O, Hagiwara Y, Hong TJ, Lih OS, Acharya UR. Deep learning for healthcare applications based on physiological signals: a review. *Comput Methods Programs Biomed* 2018;161:1–13. <https://doi.org/10.1016/j.cmpb.2018.04.005>.
- [66] Haykin SS. *Neural networks: a comprehensive foundation*. 1999.
- [67] Gershenson C. *Artificial Neural Networks for Beginners*. Arxiv Prepr Cs/0308031 2003. p. 1–8.
- [68] Lecun Y, Bengio Y, Hinton G. Deep learning. *Nature* 2015;521:436–44. <https://doi.org/10.1038/nature14539>.
- [69] Yıldırım Ö, Plawiak P, Tan RS, Acharya UR. Arrhythmia detection using deep convolutional neural network with long duration ECG signals. *Comput Biol Med* 2018;102:411–20. <https://doi.org/10.1016/j.compbmed.2018.09.009>.
- [70] Plawiak P, Acharya UR. Novel deep genetic ensemble of classifiers for arrhythmia detection using ECG signals. *Neural Comput Appl* 2019. <https://doi.org/10.1007/s00521-018-03980-2>.
- [71] Acharya UR, Oh SL, Hagiwara Y, Tan JH, Adam M, Gertych A, et al. A deep convolutional neural network model to classify heartbeats. *Comput Biol Med* 2017;89:389–96. <https://doi.org/10.1016/j.compbmed.2017.08.022>.
- [72] Oh SL, Ng EYK, Tan RS, Acharya UR. Automated diagnosis of arrhythmia using combination of CNN and LSTM techniques with variable length heart beats. *Comput Biol Med* 2018;102:278–87. <https://doi.org/10.1016/j.compbmed.2018.06.002>.
- [73] Baloglu UB, Talo M, Yildirim O, Tan RS, Acharya UR. Classification of myocardial infarction with multi-lead ECG signals and deep CNN. *Pattern Recogn Lett* 2019;122:23–30. <https://doi.org/10.1016/j.patrec.2019.02.016>.
- [74] Acharya UR, Fujita H, Sudarshan VK, Oh SL, Adam M, Koh JEW, et al. Automated detection and localization of myocardial infarction using electrocardiogram: a comparative study of different leads. *Knowledge-Based Syst* 2016;99:146–56. <https://doi.org/10.1016/j.knsys.2016.01.040>.
- [75] Fujita H, Cimr D. Computer Aided detection for fibrillations and flutters using deep convolutional neural network. *Inf Sci (Ny)* 2019;486:231–9. <https://doi.org/10.1016/j.ins.2019.02.065>.
- [76] Acharya UR, Fujita H, Lih S, Raghavendra U, Hong J. Automated identification of shockable and non-shockable life-threatening ventricular arrhythmias using convolutional neural network. *Futur Gener Comput Syst* 2018;79:952–9. <https://doi.org/10.1016/j.future.2017.08.039>.
- [77] Tan JH, Hagiwara Y, Pang W, Lim I, Oh SL, Adam M, et al. Application of stacked convolutional and long short-term memory network for accurate identification of CAD ECG signals. *Comput Biol Med* 2018;94:19–26. <https://doi.org/10.1016/j.compbmed.2017.12.023>.
- [78] Ngo LH. Using a deep learning network to diagnose congestive heart failure. *Radiology* 2018;182341. <https://doi.org/10.1148/radiol.2018182341>.